SLAC-PUB-12438
April 2007

Storage Ring Optics Measurement, Model, and Correction

Yiton T. Yan
SLAC, 2575 Sand Hill Road, Menlo Park, CA 94025, USA

1 Introduction

To improve the optics of a storage ring, it is very helpful if one has an accurate lattice model. Although the ideal lattice may serve such a purpose to some extent, in most cases, real accelerator optics improvement requires accurate measurement of optics parameters. In this section, we present precision measurements of a complete set of linear orbits from which we can form a linear optics model to match the linear optics of the real machine. We call such a model a virtual machine [1].

To obtain a virtual machine, one starts with a computer lattice model with its initial state of the ideal lattice design or the previously obtained virtual machine. A complete set of independent machine quantities must be considered as variables to fit a sufficient set of well chosen linear-optics parameters that are obtainable from calculation of the computer lattice model and measurement of the real machine. It can be better interpreted with a simple mathematical formula,

$$\vec{Y}\left(\vec{X}\right) = \vec{Y}_m \tag{1}$$

where the array $\vec{X}$ represents a complete set of variables while array $\vec{Y}$ is a well selected sufficient set of optics parameters that are to be fitted to their respective corresponding quantities, the array $\vec{Y}_m$, from real machine measurements.

$\vec{Y}$ is the response to $\vec{X}$ and is therefore a vector function of $\vec{X}$ as is explicitly shown in Equation (1). The task is to find $\vec{X}$ such that $\vec{Y}$ matches $\vec{Y}_m$. For linear geometric optics, a reasonably complete set of independent variables would be all quadrupole strengths and sextupole feed-downs. Since we cannot avoid BPM gains and BPM cross couplings, they should also be included as variables. The response quantities we have chosen are the phase advances and the Green's functions among BPMs. The Green's functions are simply the transfer matrix components R_{12}, R_{34}, R_{32}, R_{14} between any two BPMs. There are essentially an unlimited number of such Green's functions that help in fitting convergence and accuracy. We can also choose Eigen coupling ellipses' tilt angles and axis ratios at all double-view BPM locations as response quantities. However, we usually leave these coupling quantities alone for an after-fitting check to see if they automatically match between the virtual machine and the real machine to make sure the virtual machine is indeed the right one.

Submitted to ICFA Beam Dynamics Newsletter

Work supported by US Department of Energy contract DE-AC02-76SF00515

The above variables and response quantities form a complete fitting system for geometric optics only. Therefore, if we include the linear dispersions at BPMs as response quantities, we should add suitable bending magnet strengths and/or orbit corrector strengths as fitting variables. However, for application to PEP-II optics, we found that once the geometric optics was fitted, the dispersion was roughly matched between the virtual model and the measurement for most cases. This encouraged us to consider adding dispersion fitting without adding bending or corrector magnet strengths as variables. However, we may turn on normal quadrupole skew components as additional variables to achieve dispersion fitting with negligible effect on the geometric optics.

Once the virtual machine is obtained, one may use it to find and adjust one or two magnets with noticeable differences from our expectation. However, a more fruitful practice would be to use the virtual machine to search for an easily-approachable better-optics model by pre-selecting and fitting a group of normal and skew quadrupole strengths or orbit correctors (for creating sextupole bumps), and then create a machine operation knob for dialing into the real accelerator. These procedures have been successfully applied to PEP-II for optics improvement and have made a major contribution to PEP-II luminosity enhancement.

2 Geometric and Chromatic Orbit Measurement with a Model-Independent Analysis (MIA)

2.1 Geometric orbit measurement

Linear geometric optics is determined if one has 4 independent linear (betatron) orbits. This can be shown by first forming the 4 independent linear orbits at each location into a 4-by-4 matrix $\boldsymbol{Z}$, such that each orbit is in a column. Then a linear map, a 4-by-4 matrix $\mathbf{R}^{ab}$, can map the orbit matrix from any point a to any other point b such that $\mathbf{Z}^b = \mathbf{R}^{ab}\mathbf{Z}^a$. Since $\mathbf{Z}^a$ has an inverse for 4 independent linear orbits, the linear map between any two points $\mathbf{R}^{ab}$ is determined. Therefore, a complete geometric set of data will have to provide the extraction of 4 independent orbits.

With a model-independent analysis (MIA) [2], ideally, one may take advantage of beam particle jittering for extracting 4 independent linear orbits with Model-Independent Analysis MIA [2] from multi-sets of turn-by-turn BPM buffer data without invading the machine. However, unfortunately and fortunately (to be clear later), this is not the case for a damping storage ring such as the PEP-II e- (HER) or e+ (LER) storage ring due to radiation damping. Therefore, for a damping storage ring one must unfortunately invade the machine to excite the betatron orbits. In order to extract 4 independent linear orbits, the most economic process would be through two orthogonal resonance excitations, one at the horizontal (Eigen-plane 1) and the other at the vertical (Eigen-plane 2) betatron tune, and then take and store buffered BPM data. Since each betatron motion has two degrees of freedom (phase and amplitude), each excitation generates a pair of conjugate (cosine- and sine-like) betatron orbits. They are obtained from the real and imaginary parts of the tune-matched (zooming) FFT respectively. Fortunately, it should be noted that exciting betatron orbits for a damping machine

makes the wanted signal (the betatron motion) stand out. Figure 1 shows an example of 4 independent linear orbits from two resonance excitations for the PEP-II Low-Energy Ring (LER). Orbits x_1, x_2, y_3, y_4 show the major projection of the betatron motions while orbits y_1, y_2, x_3, x_4 show strong linear couplings in the interaction region (IR). Each pair of the conjugate orbits (x_1, x_2) and (y_3, y_4) contains the phase advancement which will be discussed later.

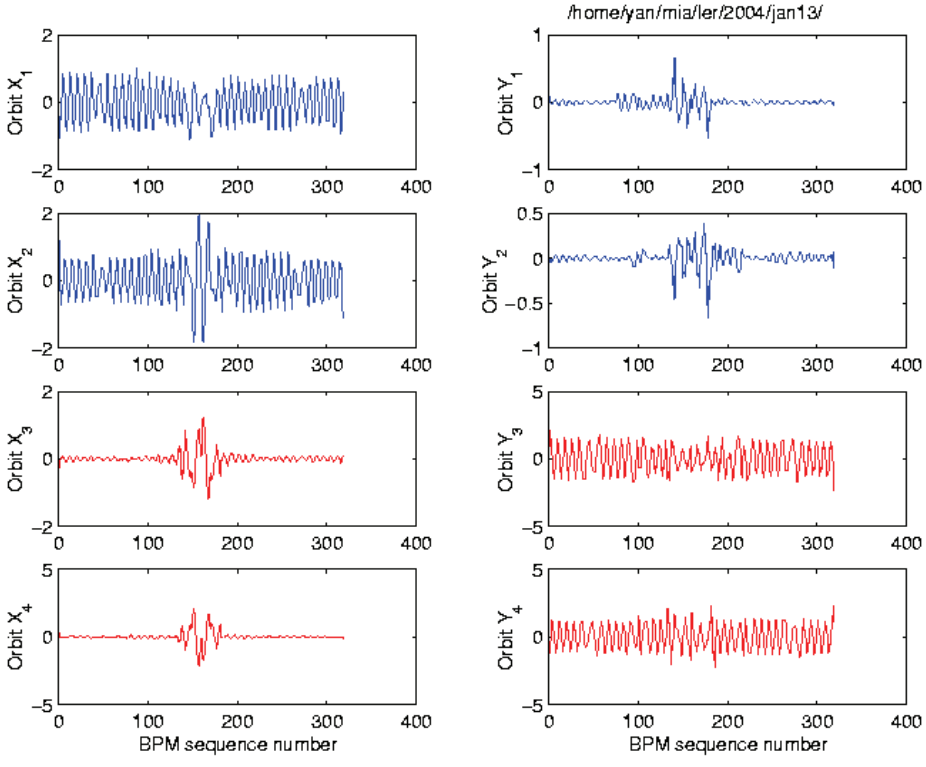

Figure 1: Four independent linear orbits extracted from PEP-II LER BPM buffer data taken on January 13, 2004. The first two orbits (x_1, y_1) and (x_2, y_2) are extracted from beam orbit resonance excitation at the horizontal tune while the other two orbits (x_3, y_3) and (x_4, y_4) are from resonance excitation at the vertical tune.

2.2 Chromatic orbit measurement

In order to extract dispersion, one may change the beam particle energy to find the transverse orbit difference. One may also try to use singular value decomposition (SVD) on the resonantly excited betatron orbits, where one may find the third largest singular mode to be the dispersion mode and the first and the second singular modes to be the two-degrees-of-freedom betatron motion modes, given that all bad BPM data have been excluded. However, to be consistent with the above accurate geometric orbit measurement, longitudinal oscillation at the synchrotron tune is resonantly excited for an additional transverse BPM data acquisition. Chromatic (dispersed) orbits at BPM locations are then measured by taking a longitudinal-tune-matched (zooming) FFT from such turn-by-turn BPM data.

2.3 Response quantities

Once the variables ($\vec{X}$ in Eq.1) in the computer lattice model are given, one can update the computer lattice transfer matrices. The response quantities ($\vec{Y}$ in Eq.1: the phase advances and the Green's functions among BPMs, Eigen coupling ellipses' tilt angles and axis ratios, and the dispersions at BPM locations), are then calculated by projection of these updated transfer matrices or the concatenated one-turn linear maps. Their corresponding quantities ($\vec{Y}_m$ in Eq.1) from measurement are described below:

2.4 Phase advances

The orbit betatron phase at each BPM location can be obtained by taking the arctangent of the ratio of the imaginary part to the real part of the resonance excitation FFT mode [1]. Phase advances between adjacent BPMs can then be calculated by subtractions. Note that the ratio of the imaginary part to the real part of the FFT will cancel the linear BPM gains but not the BPM cross couplings because beam orbit couplings and BPM cross couplings are not distinguishable from measurement. Therefore the phase advances among BPMs are repeatedly calculated during the Least Square fitting process as the BPM cross couplings and BPM gains are updated to correct the linear orbits.

2.5 Linear Green's functions

The linear Green's functions [3] are simply R_{12}^{ab}, R_{14}^{ab}, R_{14}^{ab}, R_{32}^{ab} of the linear transfer matrix between any two BPMs labelled as *a* and *b*. They can be derived from the 4 independent orbits as given below.

$$\left(x_1^a x_2^b - x_2^a x_1^b\right)/Q_{12} + \left(x_3^a x_4^b - x_4^a x_3^b\right)/Q_{34} = R_{12}^{ab}$$
$$\left(x_1^a y_2^b - x_2^a y_1^b\right)/Q_{12} + \left(x_3^a y_4^b - x_4^a y_3^b\right)/Q_{34} = R_{32}^{ab}$$
$$\left(y_1^a x_2^b - y_2^a x_1^b\right)/Q_{12} + \left(y_3^a x_4^b - y_4^a x_3^b\right)/Q_{34} = R_{14}^{ab}$$
$$\left(y_1^a y_2^b - y_2^a y_1^b\right)/Q_{12} + \left(y_3^a y_4^b - y_4^a y_3^b\right)/Q_{34} = R_{14}^{ab}$$

where Q_{12} and Q_{34} are the two betatron motion invariants of the two transverse resonance excitation at equilibrium state. If there is no BPM error, the two invariants and the Green's functions can be accurately derived from the 4 independent linear orbits. However, before Eq.1 is fitted and thus the BPM gains and cross couplings are not determined, we can only determine the ratio of the two invariants [4] and therefore leave either Q_{12} or Q_{34} as a fitting variable that belongs to $\vec{X}$ in Eq.1. On the other hand, if we have all double-view BPMs, we could update the 4 independent orbits and therefore update the Green's functions each time we update the invariants, the BPM gains, and BPM Cross couplings during the fitting process. However, in most cases, one may not have all double-view BPMs. Therefore, we consider fitting these Green's functions in the BPM measurement space. That is, we transform corresponding Green's

functions calculated from the computer lattice model into the BPM measurement space for Green's function fitting. The transformation is given below.

$$R_{12} = g_x^b R_{12} g_x^a + g_x^b R_{14} \theta_{xy}^a + \theta_{xy}^b R_{32} g_x^a + \theta_{xy}^b R_{34} \theta_{xy}^a$$
$$R_{32} = g_y^b R_{32} g_x^a + g_y^b R_{34} \theta_{xy}^a + \theta_{yx}^b R_{12} g_x^a + \theta_{yx}^b R_{14} \theta_{xy}^a$$
$$R_{14} = g_x^b R_{14} g_y^a + g_x^b R_{12} \theta_{yx}^a + \theta_{xy}^b R_{34} g_y^a + \theta_{xy}^b R_{32} \theta_{yx}^a$$
$$R_{34} = g_y^b R_{34} g_y^a + g_y^b R_{32} \theta_{yx}^a + \theta_{yx}^b R_{14} g_y^a + \theta_{yx}^b R_{12} \theta_{yx}^a$$

where the BPM gains, $g_x^a, g_x^b, g_y^a\, g_y^b$, and the BPM cross coupling multipliers, $\theta_{xy}^a, \theta_{xy}^b, \theta_{yx}^a, \theta_{yx}^b$, are repeatedly updated and applied for making the transformation during the fitting process.

2.6 Coupling ellipses

For each double-view BPM, one can trace the MIA extracted high-resolution real-space orbits to obtain a coupling ellipse in real space for each resonance (Eigen) excitation. Shown in Figure 2 are typical Eigen ellipses projected in the real X-Y plane.

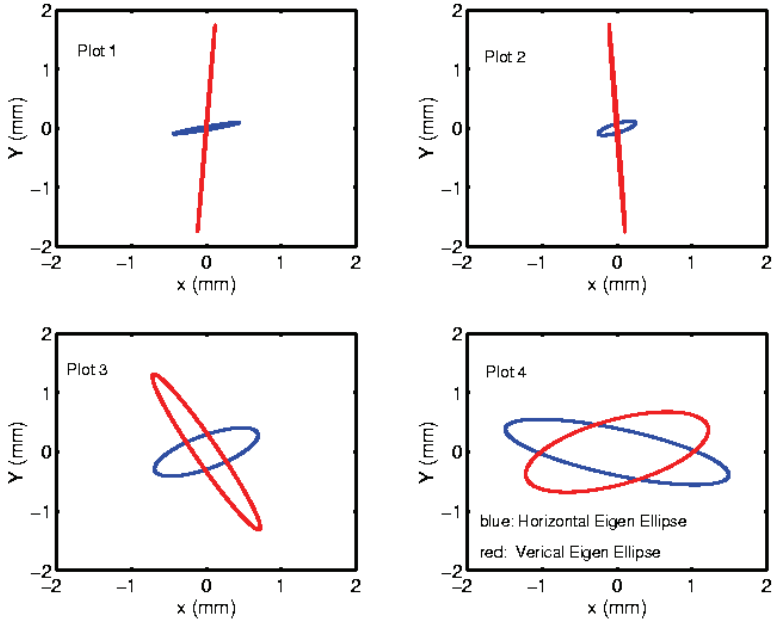

Figure 2: Eigen-mode coupling ellipses projected on the transverse x-y plane at 4 double-view BPM locations of PEP-II LER. The top 2 are at the two BPMs beside the IP, which show little coupling, while the bottom 2 are at the tenth BPMs from IP in each side, which show large couplings as the axis ratios of the short axis vs the long axis are large. (data acquired on September 30, 2003).

Therefore, one can calculate coupling ellipse tilt angles and axis ratios for all double-view BPMs [5]. The tilt angle of the coupling ellipse at the IP for the horizontal Eigen resonance excitation is very close to the real tilt angle of the beam at the IP. One

can also calculate these corresponding coupling parameters from the linear map of a lattice model [5]. Therefore, these quantities can be used as part of the fitting parameters to help obtain an accurate virtual machine. For fitting speed consideration, we prefer using more Green's functions to using coupling ellipses' tilt angles and axis ratios. However, these coupling ellipses' tilt angles and axis ratios are still very useful for after-fitting checks of self consistency that would verify the fitting accuracy.

2.7 Dispersions

Once we obtain the chromatic orbits from the longitudinal oscillation excitation, we can treat the chromatic orbits as being proportional to the linear dispersions. Both horizontal and vertical dispersions have the same proportional constant δ that is to be determined. That is, δ is a variable which belongs to $\vec{X}$ in Eq.1.

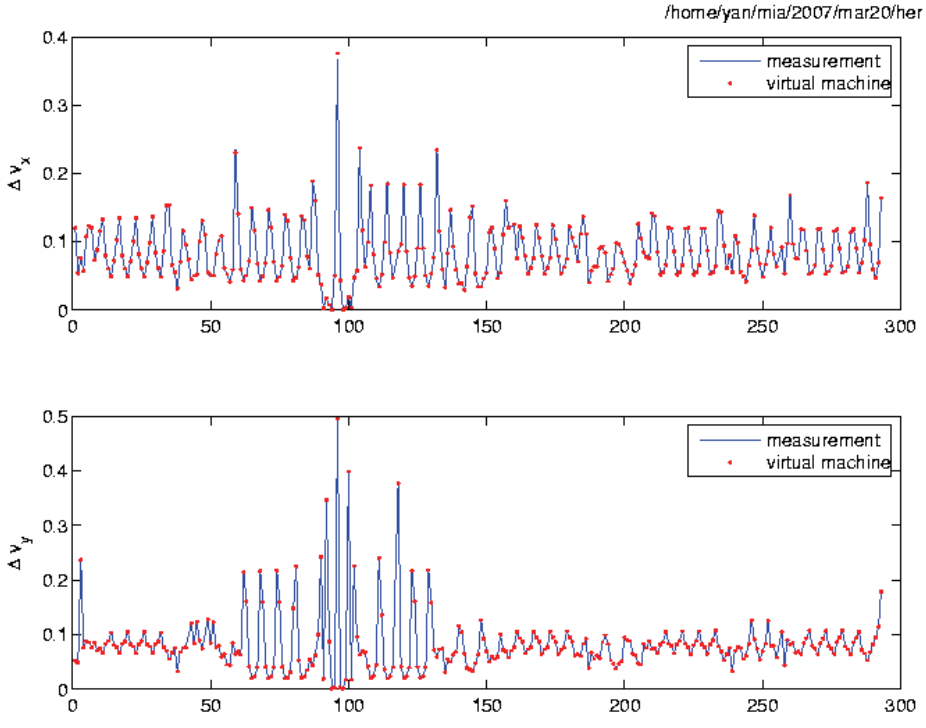

Figure 3: Typical plots comparing phase advances from measurement (blue) and from the virtual machine (red) of PEP-II HER on March 20, 2007.

3 SVD-Enhanced Least-Squares Fitting

Each time the variables $\vec{X}$ (all quadrupole strengths, all sextupole feed-downs, all BPM gains and BPM cross couplings, one invariant, and one dispersion proportional constant) in Eq.1 are updated from the computer lattice model, one can calculate and

update the phase advances, the Green's functions and the dispersions so as to fit them to their respective corresponding quantities derived from the 4 independent orbits that are obtained through high-resolution MIA analysis of the turn-by-turn BPM buffer data. With reasonable guessed initial values for the variables (for example, initialization with the ideal lattice design or with the previous virtual machine), Eq.1 can be efficiently carried out with an SVD-enhanced least-square fitting [6] that guarantees convergence provided that all bad BPM data are excluded. Figure 3 shows a comparison of phase advances between measurement and the corresponding virtual machine for PEP-II HER. Since the phase advances are the fitted response quantities, that they match very well is a necessary but not necessarily sufficient condition to guarantee an accurate virtual machine. Fortunately, as stated in Subsection 2.6, for fitting speed consideration, we do not fit for the coupling ellipses' parameters; we reserve them for after-fit check. Their automatic matching without fitting can establish a much stronger condition to make sure the fitting is all right. Figure 4 shows a comparison of coupling ellipses' parameters between measurement (blue) and the corresponding SVD-enhanced Least-Square fitted PEP-II LER virtual machine (red). The strong match shows that the fitting is pretty accurate and the virtual machine is reliable.

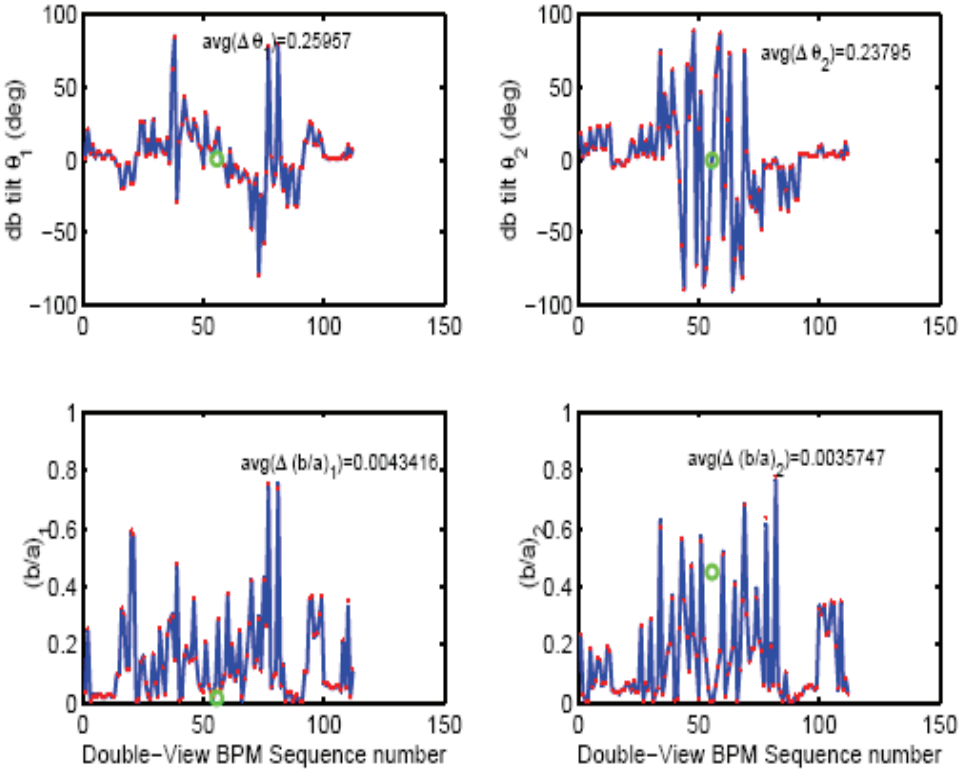

Figure 4: Typical plots comparing coupling characteristics for the whole ring. The Eigen-mode coupling ellipses' tilt angles (top plots) and axis ratios (bottom plots) are compared between measurement (blue) and its corresponding virtual machine (red) at all double-view BPM locations. Note that the left plots are for Eigen mode 1 (horizontal resonance excitation) while the right plots are for Eigen mode 2 (vertical resonance excitation).

4 Application for PEP-II Measurements

The PEP-II Low-Energy Ring (LER) has 319 BPMs while the High-Energy Ring (HER) has 293 BPMs. For each measurement of the LER (or HER), we take 3 sets of the MIA data for horizontal (Eigen mode 1), vertical (Eigen mode 2), and longitudinal resonance excitation of the beam motion. Once the complete sets of MIA data are collected, we retrieve the 4 independent geometric orbits and the chromatic orbits as discussed in Section 2. At the same time, we rank BPM data validity and identify those that must be excluded from the fitting for the virtual machine. This is a key step for successful fitting – fitting unreliable data just does not work! To identify bad BPMs, we start by taking a singular value decomposition of each set of data and then identify those BPMs whose data show low correlation with most of the BPM data. At this stage, we would exclude those identified bad BPMs from the 4 independent orbits and start SVD-enhanced Least-Square fitting. In many cases, we get an accurate virtual machine without trouble. However, in some cases, we find that the residuals are not small enough after fitting is completed. In such cases, we would first find a small group of BPMs which are suspiciously bad but not identified, then take one such BPM out at a time and calculate (not fitting) its influence on the reduction of the residuals. If necessary, we would use more Green's functions in such fast tests of residual reduction. We would take out those (could be just one) BPMs that have a large effect on the residuals and continue the fitting process. Not only would we fit the residuals to a satisfactory small value such that fitted response quantities match very well, but we would also check and compare the measurement and the virtual machine for those response quantities that are not used for fitting to see if they match automatically as discussed in Section 3. Figure 5 shows a typical measurement of PEP-II HER on March 20, 2007. This figure shows a quick survey of the virtual machine optics that matches the real machine optics. It should be noted that in many cases we also try to understand the real machine optics by direct measurement without obtaining the virtual machine. However, these direct measurements rely on the perfection of BPMs and therefore are less accurate than those derived from the virtual machine because the virtual machine also takes into account the BPM gains and cross couplings.

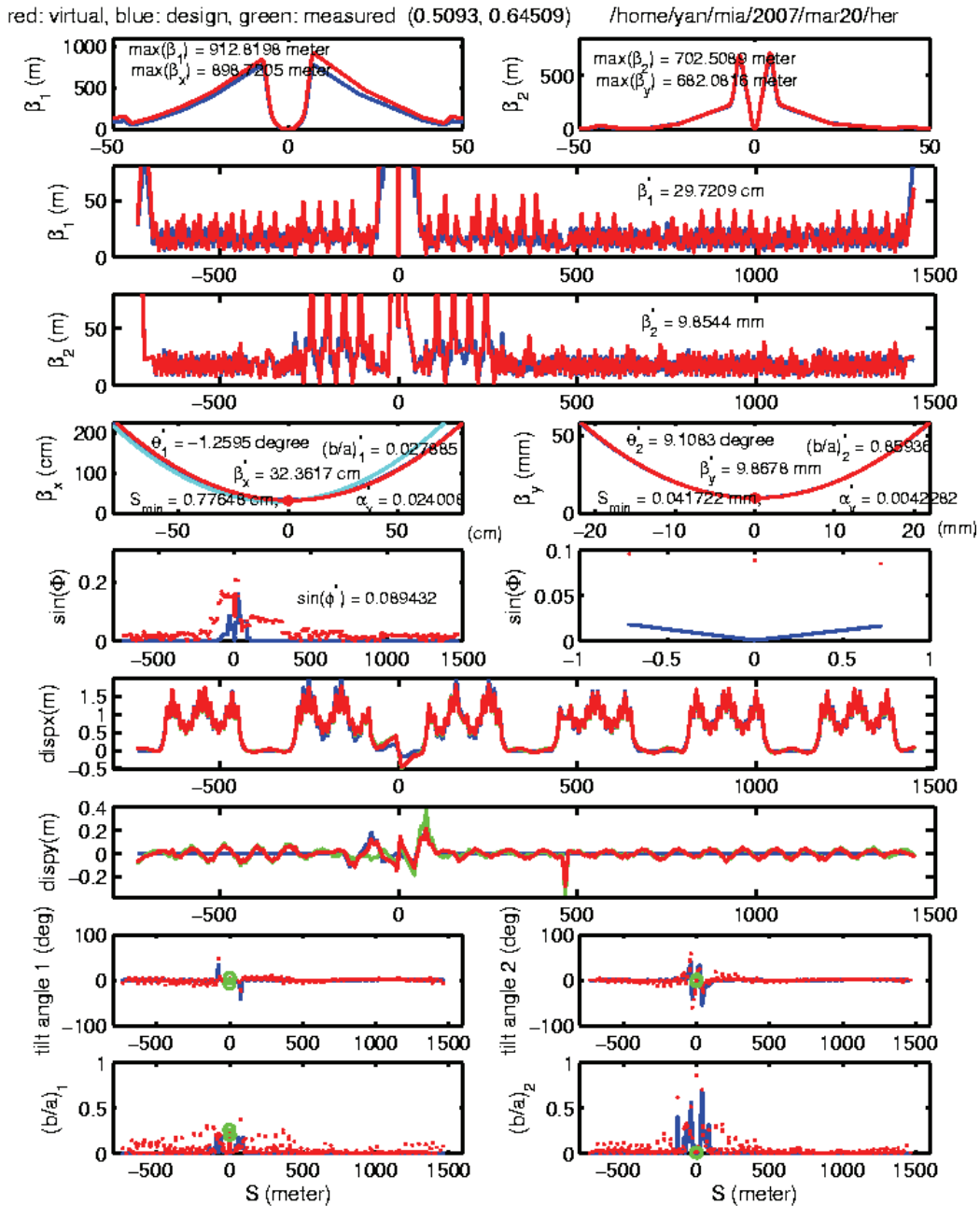

Figure 5: Typical plots to show virtual machine linear optics characteristics (red color) compared with those of the designed lattice (blue color). In this case, it is PEP-II HER measured on March 20, 2007. The top two plots show the two Eigen β functions in the vicinity of the IP followed by two plots that show the β functions for the whole machine and then the β function plots at IP, which are accompanied by prints of the β^*, α^*, Eigen ellipses' tilt angles θ^* and axis ratios $(b/a)^*$ as well the waist shifts. The next two plots show the phase-space coupling determinants sin(ϕ) followed by 2 plots that show the horizontal and vertical dispersions. The coupling ellipse parameters, the tilt angles, and the axis ratios for all double-view BPMs are compared in the last (bottom) 4 plots.

5 Application to PEP-II Optics Improvement - Examples

Once the optics-matched virtual machine is obtained through an SVD-enhanced Least-Square fitting, the updated transfer matrices can be concatenated into one-turn maps at the desired locations for calculating optics parameters. By fitting a well selected set of normal and skew quadrupoles as well as orbit correctors (for sextupole bumps), one can also find solutions for improving the optics, such as reducing the beta beating and the linear coupling, optimizing beta functions at the IP, bringing the working tune to near half integer, and improving dispersion. Furthermore, the updated virtual machine is stored online (the online model) for better subsequent online measurement. They are also fed to the program MAD to help lattice improvement and to the program LEGO for beam-beam simulations [7].

5.1 Beta beat fix

Shown in Figure 6 is the PEP-II HER β function on Nov. 22, 2005, which shows a high beta beat and was subsequently corrected through a solution from the MIA virtual model.

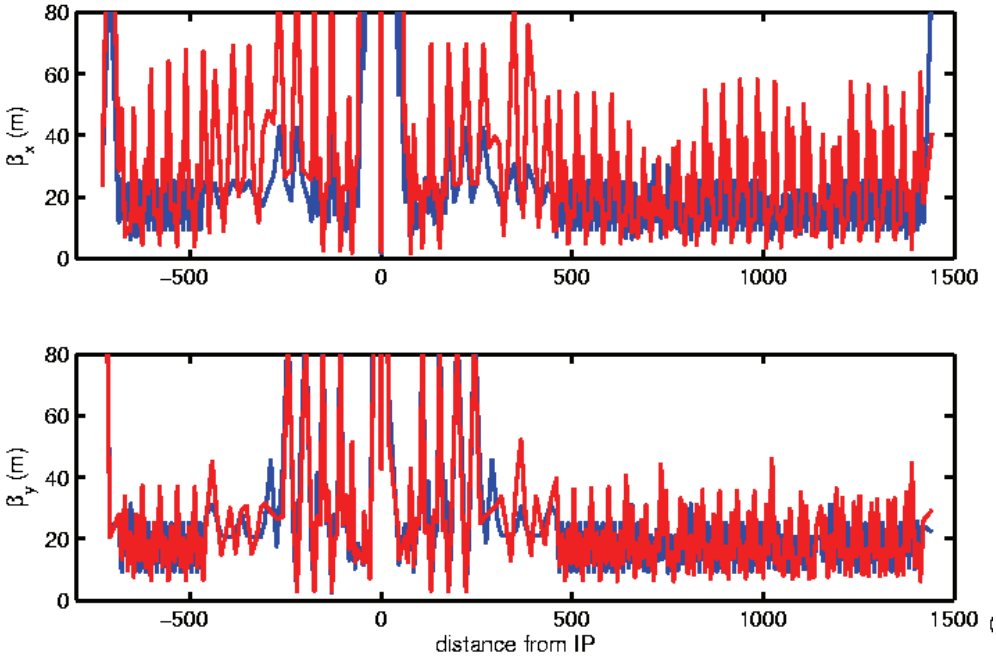

Figure 6: Comparison of PEP-II HER β functions on Nov. 22, 2005: the ideal lattice (blue color) and the virtual machine (red color). The PEP-II HER showed high beta beats which were subsequently corrected through solution from the virtual machine.

Shown in Figure 7 is the PEP-II HER β function on Mar. 16, 2006, which shows that the beta beat has been much improved. From the MIA virtual machine, we have been able to identify a key quadupole (QF5L). This normal quadrupole along with the linear trombone quads and local and global skews are used as variables in the MIA

program for finding the solution from the virtual machine. The solution is then translated into a control system knob for dialing into the PEP-II HER.

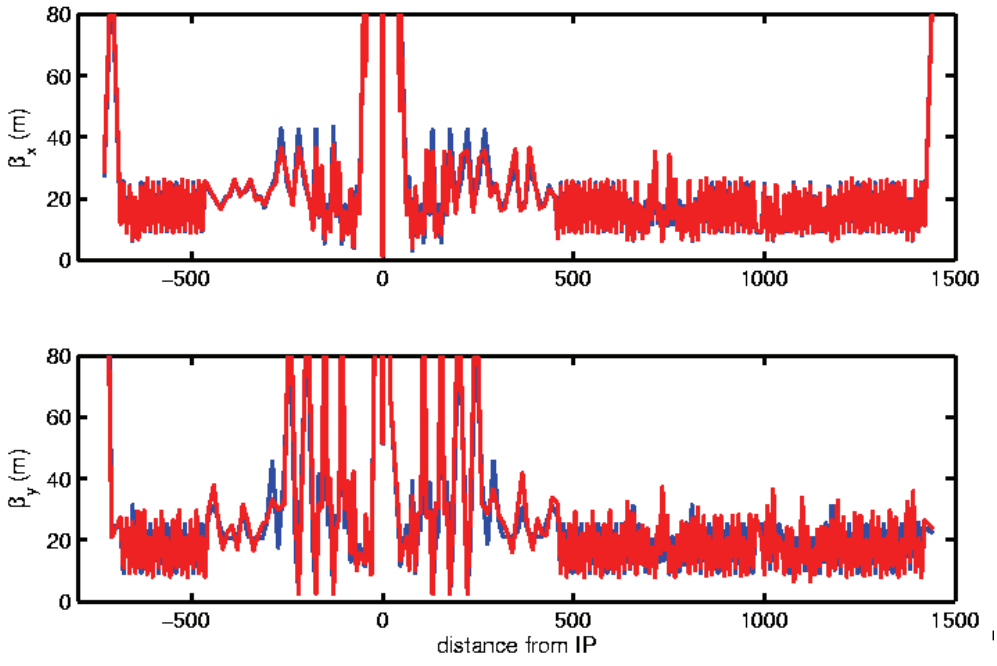

Figure 7: Comparison of PEP-II HER β functionson Mar. 16, 2006: the ideal lattice (blue color) and the virtual machine (red color). Beta beat shown in Fig. 5 has been much improved. This beta beat fix was done with a scheduled 1-shift MD.

5.2 Dispersion beat fix

As mentioned above, we have been able to include dispersion measurements in the virtual machine without adding new types of variables. Figure 8 compares dispersion calculated from the virtual machine and derived from the direct measurement of PEP-II HER on Nov. 22, 2005. There is no bending magnet or orbit corrector involved in the fitting for the virtual machine. The vertical dispersion beat was subsequently improved with the MIA virtual model.

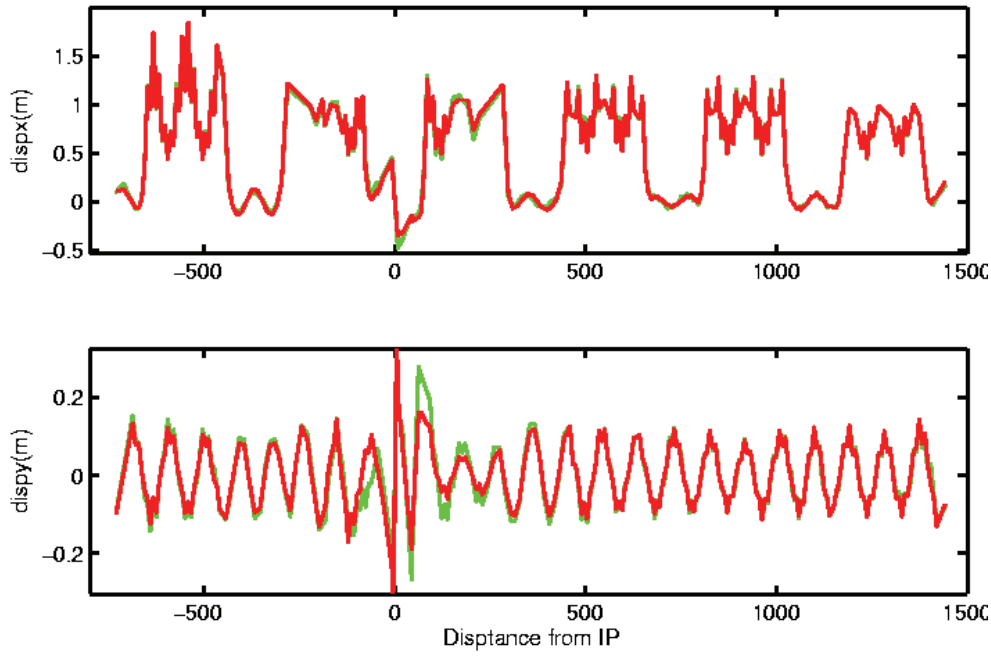

Figure 8: Comparison of PEP-II HER dispersion on Nov. 22, 2005: the direct measurement (green color) and the virtual machine. No bending magnet or orbit corrector was added as a variable for fitting. The vertical dispersion beats were subsequently fixed.

5.3 Dramatic change of machine working tunes

The MIA virtual machine has also been applied to PEP-II LER on April 29, 2003, bringing its working tune to near half integer, fixing its strong beta beat, and along with other efforts, subsequently boosting PEP-II luminosity by 50%.

5.4 Optics fix after major orbit steering

As another example, due to strong coupling in the IR, PEP-II LER major orbit steering is usually accompanied by a much degraded linear optics due to the change of sextupole feed-downs, which has been very difficult to correct. Indeed, without help from an accurate optics model, there have been many previous tries of LER major orbit steering which ended with back-out. With an accurate MIA virtual machine established for the LER (right after the major steering), we have been able to correct the linear optics such that the major LER orbit steering in April, 2006 was kept. Figure 9 shows the LER linear coupling characteristics after dialing in MIA solutions right after the major orbit steering. This PEP-II LER coupling is a record low with a record low residual from the ideal lattice.

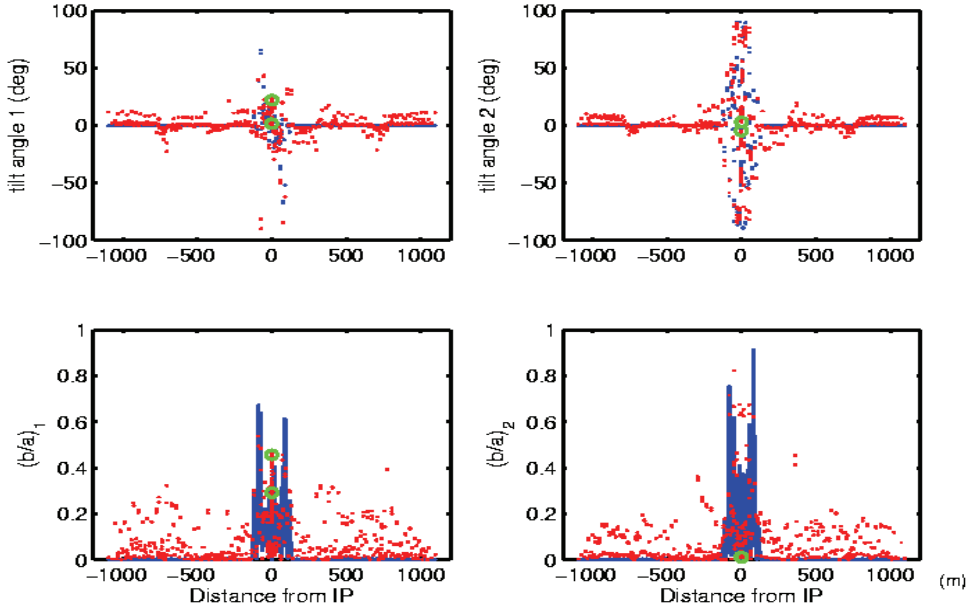

Figure 9: Comparison of PEP-II LER linear couplings on Apr. 21, 2006: the ideal lattice (blue color) and the virtual machine (red color). This was after a major orbit steering that was accompanied by a MIA solution for linear optics correction. Top plot shows the Eigen ellipse tilt angles while the bottom plot shows the Eigen ellipse axis ratios for Eigen plane 1 and 2 respectively

5.5 Virtual emittance and virtual luminosity

The beta beat fix example shown in Figure 7 was achieved with a formal schedule of 1 shift of machine development (MD). Here we show another example without a formal MD schedule. That is, we tried to dial in the MIA solution knob to HER adiabatically during PEP-II collision. Figure 10 shows the strong beta beat from the MIA virtual machine of PEP-II HER on Feb 6, 2007. Based on this virtual machine, we found a solution that would significantly reduce the beta beat. We had the chance to adiabatically dial 50% of the solution into the real machine, HER, during collision. Subsequently, the beta beat was reduced by half as shown in Figure 11, while the emittance was improved as shown in Table 1. To make up the other 50% solution that was not dialed into the machine, we tried to get another solution, which we called the new half solution, from the updated virtual machine on Feb. 8, 2007 after 50% of the solution derived from the virtual machine of Feb. 6, 2007 was in. The beta beat is expected to be nicely fixed as shown in Figure 12, which shows the beta functions of the wanted model for the new half solution. The X emittance can also be nicely reduced to near the ideal lattice design of about 50 nm as shown on Table 1. However, before the machine changed (drifts) enough such that the new half solution was no longer suitable, we did not get a chance to dial in the new half solution in time. Therefore we do not know if this new half solution will indeed work as expected.

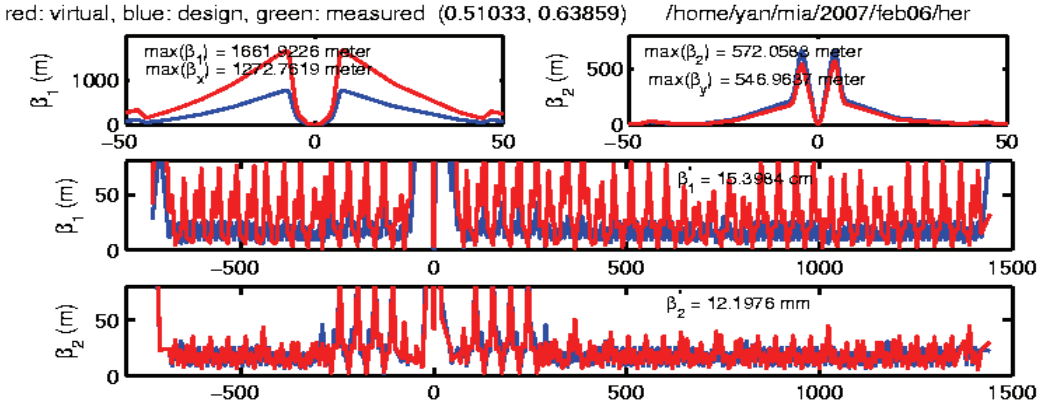

Figure 10: Comparison of PEP-II HER β function on Feb. 6, 2007: the ideal lattice (blue color) and the virtual machine (red).

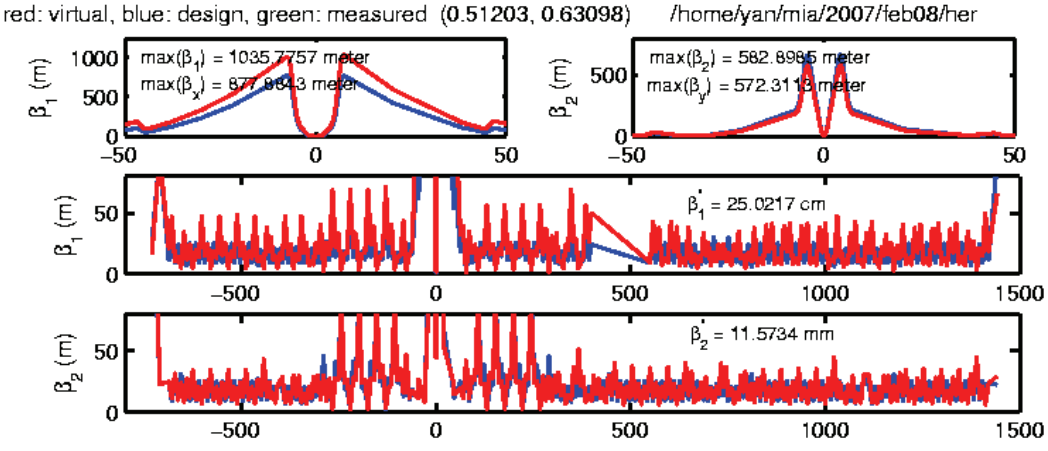

Figure 11: Comparison of PEP-II HER β function on Feb. 8, 2007 after dialing in 50% of the MIA solution knob derived from the virtual machine of Feb. 6, 2007: the ideal lattice (blue color) and the virtual machine (red).

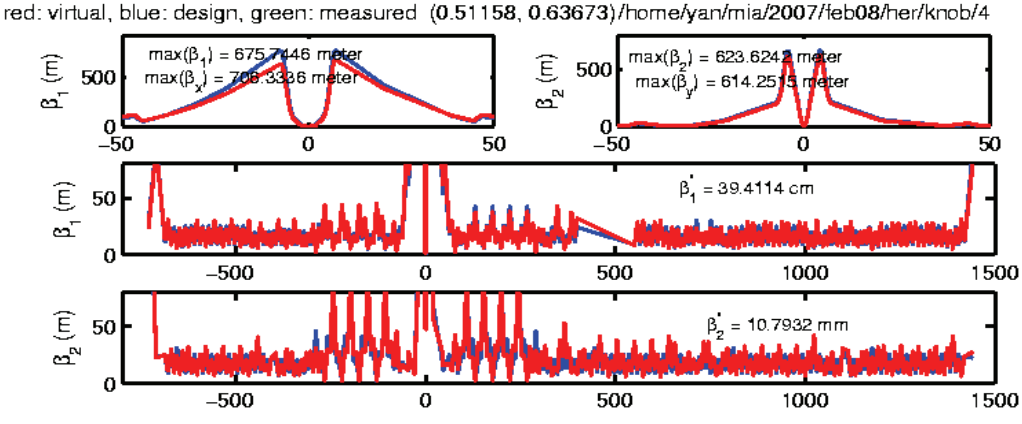

Figure 12: Comparison of PEP-II HER β function on Feb. 8, 2007: the ideal lattice (blue color) and the wanted model (red color) for the new half solution derived from the virtual machine of Feb. 8, 2007.

Table 1: Emittance comparison for PEP-II HER

PEP-II HER	X emittance (nm)	Y emittance (nm)
Virtual HER Feb. 6, 2007	94	0.59
Virtual HER Feb. 8, 2007 (after 50% MIA solution in)	64	0.24
Wanted model for the new half solution derived from Virtual HER Feb. 8, 2007 after 50% MIA solution	52	0.24
Ideal Lattice emittance calculated from MIA program	51	0.13

Since we can get the virtual machine if we extract the MIA BPM buffer data from the real machine, we can calculate in detail how the emittance is integrated through the circumference. In Figure 13, the top plot shows how the X emittance is integrated through the circumference while the bottom plot shows how the Y emittance is integrated through the circumference.

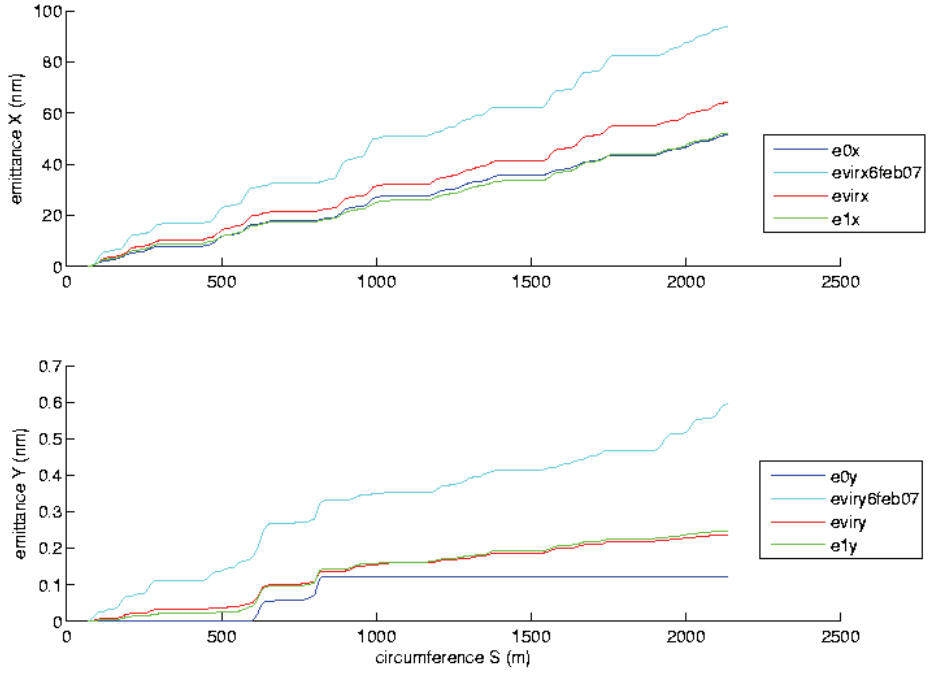

Figure 13: Comparison of PEP-II HER X emittance (top plot) and Y emittance (bottom plot) contribution through circumference for the virtual machine on Feb 6, 2007 (evirx6feb07, eviry6feb07), the virtual machine on Feb 8, 2007 (evirx, eviry), the wanted model for the new half solution derived from the virtual HER on Feb 8, 2007 (e1x, e1y), and the ideal lattice of HER (e0x, e0y).

It should also be noted that since we can calculate the emittance and the IP optics parameters from the virtual machines (HER and LER), we can calculate the virtual

specific luminosity and the virtual luminosity of PEP-II given that we get both virtual LER and virtual HER.

6 Conclusions

We have used a model-independent analysis (MIA) for accurate orbit and phase advance measurement and then used an SVD-enhanced Least Square fitting for building accurate virtual models for PEP-II e+, e- storage rings. The MIA virtual machine matches very well the real-machine linear optics including dispersion. It has successfully improved PEP-II beta beats, linear couplings, half-integer working tunes, and dispersion. The success comes from:

- **Auto optimized selection of the Eigen modes for the SVD-enhanced Least-Square fitting**: The auto optimized SVD-enhanced Least-Square fitting can avoid degeneracy and has a fairly fast convergence rate allowing for application to a fairly large system.
- **PEP-II ring has a reasonable amount of good BPMs:** The PEP-II ring has a reasonable amount of good BPMs allowing for extraction of sufficient physical quantities for fitting.
- **Essentially unlimited Green's functions add to fitting convergence:** The linear Green's functions among BPMs can provide essentially unlimited fitting constraints that add significantly to convergence and accuracy.

Acknowledgement

The author would like to thank Y. Cai, A. Chao, W. Colocho, F-J. Decker, S. Ecklund, J. Irwin, S.Y. Lee, J. Seeman, M. Sullivan, J. Turner, C-x. Wang, U. Wienands, W. Wittmer, M. Woodley, and J. Yocky for their collaboration and many helpful discussions.

References

1. Y.T. Yan, Y. Cai, F-J. Decker, S. Ecklund, J. Irwin, J. Seeman, M. Sullivan, J. Turner, U. Wienands, “Virtual Accelerator for Accelerator Optics Improvement”, SLAC-PUB-11209, in PAC2005 Proceedings (2005), MPPE058.
2. J. Irwin, C.X. Wang, Y.T. Yan, etc. “Model-Independent Beam-Dynamics Analysis”, Phys. Rev. Lett., **82**, 1684 (1999).
3. J. Irwin, and Y.T. Yan, “Beamline model verification using model-independent analysis”, SLAC-PUB-8515 (2000), in EPAC2000 Conference Proceedings.
4. Y.T. Yan, Y. Cai,, W. Colocho, F-J. Decker, to be presented in PAC2007.
5. Y.T. Yan and Y. Cai, “Precision measurement of coupling Eigen ellipses in a storage ring,” SLAC-PUB-10371 (2006).
6. Y.T. Yan and Y. Cai,, “Precision PEP-II optics measurement with an SVD-enhanced Least-Square fitting”, Nucl. Instrum. Meth. A555:336-339, 2006.
7. Y. Cai, et al., “Luminosity improvement at PEP-II based on optics model and beam-beam simulation”, in EPAC2006 proceedings: MOPLS052.